ISSN 1063-7729, Astronomy Reports, 2010, Vol. 54, No. 12, pp. 1105–1124. © Pleiades Publishing, Ltd., 2010.
Original Russian Text © M.K. Abubekerov, N.Yu. Gostev, A.M. Cherepashchuk, 2010, published in Astronomicheskiĭ Zhurnal, 2010, Vol. 87, No. 12, pp. 1199–1220.

Light Curve Analysis for Eclipsing Systems with Exoplanets. The System HD 209458

M. K. Abubekerov, N. Yu. Gostev, and A. M. Cherepashchuk

Sternberg Astronomical Institute, Moscow State University, Universitetskii pr. 13, Moscow, 119992 Russia

Received May 31, 2010; in final form, July 1, 2010

Abstract—We have analyzed precision light curves for HD 209458, a binary with an exoplanet. The parameters obtained at different epochs and different wavelengths are in good mutual agreement when confidence regions are used to calculate the uncertainty intervals. We demonstrate the effectiveness and reliability of our new method for estimating the uncertainty intervals. Reliable estimates are provided for the linear and quadratic limb-darkening coefficients of the star and their confidence intervals (uncertainties). We find that the wavelength dependence for the limb-darkening coefficients at $\lambda = 3201-9708$ Å differs significantly from the corresponding theoretical relation based on thin model stellar atmospheres.

DOI: 10.1134/S1063772910120048

1. INTRODUCTION

Light curves with unique precision for exoplanet transits across stars have been obtained during recent years (cf., for instance, [1–4]) thanks to various space missions (HST, CoRoT, Kepler).

Brown et al. [1] presented an analysis of an HST light curve obtained for HD 209458 in 2000. An analysis of multicolor HST light curves for this object obtained in 2003 was performed by Knutson et al [2]. The radii of the exoplanet and star, orbital inclination, and the stellar limb-darkening coefficients were determined in both studies. The most detailed study of a series of HST observations is that of Southworth [5], who derived these same parameters for various limb-darkening laws. As often happens in practical cases, the very high precision of the observations, on one hand, enabled Southworth [5] to derive the most reliable parameters for the binary, but, on the other hand, led to certain difficulties in interpreting the observations. First, the central values of the geometrical parameters of the model found for the different wavelengths, λ, demonstrated a considerable scatter, appreciably larger than the parameter uncertainties estimated using the Monte Carlo technique. Second, the geometrical parameters derived via light curve analyses for different epochs do not quite agree within the errors.

These difficulties are not due to the specific properties of the applied model, since the results obtained from the high-accuracy light curves of HD 209458 using different models (two spherical stars [6] and two biaxial ellipsoids [5, 7, 8]) agree well.

These difficulties are most likely due to the fact that Southworth [5] estimated the uncertainties of the resulting parameters using the Monte Carlo method, which is known (see, for instance, [9–12]) to provide only "internal" uncertainties (those reflected by the statistics of the normal distribution of the obtained central parameter values under the strict assumption that the model is perfectly correct), which can be too low by a factor of three to five [9].

For this reason, we undertook a new analysis of the high-precision light curves of HD 209458 from [1, 2]. We estimated the parameter uncertainties using both the differential-correction and confidence-region methods (see, for example, [13]). This latter method uses the statistics of the "external" distribution of the observed data points for the light curve generated by these normally distributed measurements—the residual functional, which depends on the square of the differences between the observed and theoretical values (a statistic distributed as χ^2_M, where M is the number of observed data points in the light curve).

In contrast to the Monte Carlo and differential-correction methods, which are equivalent [11, 12], the searches for the central parameter values and their uncertainties using confidence regions are both carried out using the same statistics (for example, a χ^2_M distribution). In this case, we estimate the "external" uncertainties of the parameters, independent of the particular distribution for the derived parameters' central values. In addition, using statistics with a χ^2_M distribution makes it possible to avoid the artificial assumption that the applied model is perfect.

By using the parameter uncertainties based on confidence regions (the "external" uncertainties), we are able to reconcile the fitting results for the multicolor light curves of HD 209458 and the light curves obtained for different epochs. We also confirm the existence of a significant discrepancy between the observed and theoretical wavelength dependences for the star's limb-darkening coefficients found in [5].

2. FITTING TECHNIQUE

We used a model with two spherical stars in a circular orbit, without reflection and ellipsoidal effects. According to data available for the exoplanet CoRoT-1b [3], whose orbital period ($P_{orb} = 1.509^{\rm d}$) is half that for the HD 209458 system ($P_{orb} = 3.52474859^{\rm d}$), the total observed amplitude of the reflection effect from the planet should not exceed $\sim 0.0001^m$, with the amplitude of the ellipsoidal effect for the optical star probably being appreciably smaller still. Consequently, brightness variations due to reflection and ellipsoidal effects will be no larger than 10^{-5} mag within the eclipse (whose duration for CoRoT-1b is ~ 0.07 of the orbital period), which is negligible. A spherical approximation for the planet seems quite satisfactory, given the uncertainty in its shape, related to the possible existence of a semitransparent atmosphere, which could be as large as $\sim 5\%$ of the planet's radius [14], possible rapid axial rotation of the planet and rotational deformation, and the small fraction of the planet that fills its Roche lobe ($\mu < 0.5$).

When calculating the light curves, we described the brightness distribution across the stellar disk using a linear limb-darkening law with the linear limb-darkening coefficient x:

$$I(\rho) = I_0 \left(1 - x + x\sqrt{1 - \frac{\rho^2}{r^2}}\right) \qquad (1)$$

and a quadratic limb-darkening law that differs from the linear law in an additional term containing the quadratic limb-darkening coefficient y:

$$I(\rho) = I_0 \left(1 - x\left(1 - \sqrt{1 - \frac{\rho^2}{r^2}}\right) - y\left(1 - \sqrt{1 - \frac{\rho^2}{r^2}}\right)^2\right). \qquad (2)$$

Here, ρ is the polar distance from the center of the stellar disk, I_0 the brightness at the disk center, and r the radius of the stellar disk. Below, we denote the brightness at the center of the disk of component 1 (the star) $I_0^{(1)}$. The brightness $I_0^{(2)}$ at the center of component 2 (the planet) and the brightness at any point of the disk of this component are assumed to be zero. Component 2 (the planet) eclipses component 1 (the star) at orbital phase $\theta = \pi$. The unit of length in our model is the distance between the centers of the star and planet $a = 1$, and the orbit is assumed to be circular. There is no "third light" in the model. The fitted model parameters are the radii of the star and planet r_1 and r_2, the orbital inclination i, the limb-darkening coefficient x_1, and, in the case of the quadratic limb-darkening law, the quadratic limb-darkening coefficient y_1.

Let us introduce the following new variables:

$$X_0^{(1)} = I_0^{(1)}(1 - x_1), \quad X_1^{(1)} = I_0^{(1)} x_1 \qquad (3)$$

for the linear limb-darkening law and

$$X_0^{(1)} = I_0^{(1)}(1 - x_1 - 2y_1), \qquad (4)$$
$$X_1^{(1)} = I_0^{(1)}(x_1 + 2y_1), \quad X_2^{(1)} = I_0^{(1)} y_1$$

for the quadratic limb-darkening law.

We can then write the brightness in the linear limb-darkening law as

$$I^{(1)}(\rho) = \left(X_0^{(1)} + X_1^{(1)}\sqrt{1 - \frac{\rho^2}{r_1^2}}\right), \qquad (5)$$

and in the quadratic law as

$$I^{(1)}(\rho) = \left(X_0^{(1)} + X_1^{(1)}\sqrt{1 - \frac{\rho^2}{r_1^2}} + X_2^{(1)}\frac{\rho^2}{r_1^2}\right). \qquad (6)$$

With these variables, the brightness at a point on the stellar disk depends linearly on $X_0^{(1)}$, $X_1^{(1)}$, and $X_2^{(1)}$, while the corresponding brightness for the nonlinear limb-darkening law differs in a single term, with the coefficient $X_2^{(1)}$. Component 2 eclipses component 1 at orbital phase $\theta = \pi$.

The total brightness of the star (component 1), equal to the total out-of-eclipse brightness of the system, is

$$L^{full} = 2\pi \int_0^{r_1} I^{(1)}(\rho)\rho d\rho \qquad (7)$$
$$= \pi r_1^2 \left(X_0^{(1)} + \frac{2}{3}X_1^{(1)}\right) = \pi r_1^2 I_0^{(1)}\left(1 - \frac{x_1}{3}\right)$$

for the linear limb-darkening law and

$$L^{full} = 2\pi \int_0^{r_1} I^{(1)}(\rho)\rho d\rho \qquad (8)$$

$$= \pi r_1^2 \left(X_0^{(1)} + \frac{2}{3} X_1^{(1)} + \frac{1}{2} X_2^{(1)} \right)$$
$$= \pi r_1^2 I_0^{(1)} \left(1 - \frac{x_1}{3} - \frac{y_1}{6} \right)$$

for the quadratic limb-darkening law.

The total brightness of the star for the quadratic limb-darkening law is

$$L^{(s)} = 2\pi \int_0^r I^{(s)}(\rho) \rho d\rho$$
$$= X_0^{(s)} \pi r_s^2 + \frac{2}{3} X_1^{(s)} \pi r_s^2 + \frac{1}{2} X_2^{(s)} \pi r_s^2, \quad s = 1, 2.$$

To make the form of the formulas used to calculate the minima of the light curve universal and reduce the number of equations, we will use the index n for the eclipsing component (nearer to the observer) and the index f for the eclipsed component (further from the observer). When actually computing the light-curve minima at orbital phases $-\pi/2 < \theta < \pi/2$ (or for $\cos\theta > 0$), the variable r_n should be changed to r_1 and r_f to r_2. The opposite change is needed for orbital phases with $\cos\theta < 0$: r_f should be changed to r_1 and r_n to r_2.

In this new notation, the brightness reduction during the eclipse is

$$L^{dec}(\Delta, r_f, r_n, X_0^{(f)}, X_1^{(f)}, X_2^{(f)}) = \iint_{S(\Delta)} I^{(f)}(S) dS, \quad (9)$$

where Δ is the distance between the disk centers and $S(\Delta)$ is the overlap area of the disks.

Following [11], we introduce the following functions to calculate the integral (9):

$$\mathcal{A}x \equiv \begin{cases} \pi, & x < -1, \\ \arccos x, & -1 \le x \le 1, \\ 0, & x > 1 \end{cases} \quad (10)$$

and

$$\mathcal{Q}x \equiv \begin{cases} \sqrt{x}, & x \ge 0, \\ 0, & x < 0, \end{cases}$$

$$\Psi(\Delta, x, y) \equiv \mathcal{A}\left(\frac{x^2 + \Delta^2 - y^2}{2x\Delta} \right),$$

$$Q(\Delta, r_f, r_n) \equiv \mathcal{Q}\left[\left(r_f^2 - (\Delta - r_n)^2 \right) \left((\Delta + r_n)^2 - r_f^2 \right) \right],$$

and also introduce polar coordinates with the origin at the center of the eclipsed star's disk and the polar angle φ increasing from the disk center of the eclipsed component, f, towards the disk center of the eclipsing component, n. Then,

$$L^{dec}(\Delta, r_f, r_n, X_0^{(f)}, X_1^{(f)}, X_2^{(f)}) \quad (11)$$
$$= \int_0^{r_f^2} \Psi(\Delta, \sqrt{\rho}, r_n) I^{(f)}(\sqrt{\rho}) d\rho$$
$$= X_0^{(f)} L_0^{dec}(\Delta, r_f, r_n) + X_1^{(f)} L_1^{dec}(\Delta, r_f, r_n) + X_2^{(f)} L_2^{dec}(\Delta, r_f, r_n).$$

The expressions for calculating L_0^{dec} and L_1^{dec} were derived in [11].

Analogous to the procedure used in [11] to derive the formula for L_0^{dec}, we find for L_2^{dec}:

$$L_2^{dec}(\Delta, r_f, r_n) = \frac{2}{r_f^2} \int_0^{r_f} \rho^3 \Psi(\Delta, \rho, r_n) d\rho \quad (12)$$
$$= \Psi(\Delta, r_f, r_n) \frac{r_f^2}{2} + \frac{r_n^2}{2r_f^2} \left(2\Delta^2 + r_n^2 \right) \Psi(\Delta, r_n, r_f) - \frac{1}{8r_f^2} \left(\Delta^2 + 5r_n^2 + r_f^2 \right) Q(\Delta, r_f, r_n).$$

The partial derivatives of L_2^{dec} are

$$\frac{\partial L_2^{dec}(\Delta, r_f, r_n)}{\partial \Delta} = \frac{2}{r_f^2} \Delta r_n^2 \Psi(\Delta, r_n, r_f) - \frac{\Delta^2 + r_n^2 + r_f^2}{2\Delta r_f^2} Q(\Delta, r_f, r_n), \quad (13)$$

$$\frac{\partial L_2^{dec}(\Delta, r_f, r_n)}{\partial r_f} = 2r_f \Psi(\Delta, r_f, r_n) - \frac{2}{r_f} L_2^{dec}(\Delta, r_f, r_n), \quad (14)$$

$$\frac{\partial L_2^{dec}(\Delta, r_f, r_n)}{\partial r_n} = \frac{2}{r_f^2} r_n \left(\Delta^2 + r_n^2 \right) \times \Psi(\Delta, r_n, r_f) - \frac{2}{r_f^2} r_n Q(\Delta, r_f, r_n). \quad (15)$$

For a circular orbit, the distance between the stellar-disk centers Δ depends on the phase θ and orbital inclination i as

$$\Delta(\theta, i) = \sqrt{\cos^2 i + \sin^2 i \sin^2 \theta}. \quad (16)$$

The binary's light curve for the model with the linear limb-darkening law is described by the function

$$L(\theta, r_1, r_2, i, X_0^{(1)}, X_1^{(1)}) \quad (17)$$
$$= X_0^{(1)} L_0^{(1)}(\theta, r_1, r_2, i) + X_1^{(1)} L_1^{(1)}(\theta, r_1, r_2, i)$$

and with the quadratic limb-darkening law by the function

$$L(\theta, r_1, r_2, i, X_0^{(1)}, X_1^{(1)}, X_2^{(1)}) \quad (18)$$
$$= X_0^{(1)} L_0^{(1)}(\theta, r_1, r_2, i) + X_1^{(1)} L_1^{(1)}(\theta, r_1, r_2, i) + X_2^{(1)} L_2^{(1)}(\theta, r_1, r_2, i).$$

Expressions needed to calculate $L_{0,1,2}^{(1)}$ were derived in [11, 12]. Note that Eq. (16) for L_2^{dec} in [12] contains an error: the coefficient $1/r_f^2$ in front of the integral is missing. Thus, Eqs. (12)–(15) here rather than (16)–(19) from [12] should be used to calculate L_2^{dec} and its derivatives.

Our models assume the total brightness L^{full} to be known (normalized to unity in the computations). Using (7), we exclude the parameter

$$X_1^{(1)} = \frac{3L^{full}}{2\pi r_1^2} - \frac{3}{2} X_0^{(1)} \quad (19)$$

in the model with the linear limb-darkening law and, using (8), we exclude the parameter

$$X_2^{(1)} = \frac{2L^{full}}{\pi r_1^2} - 2X_0^{(1)} - \frac{4}{3} X_1^{(1)} \quad (20)$$

in the model with the quadratic limb-darkening law. Substituting (19) and (20) into (17) and (18), respectively, we obtain equations for the light curves, with the total brightness of the system being fixed:

$$L(\theta, r_1, r_2, i, X_0^{(1)}) \quad (21)$$
$$= \frac{3L^{full}}{2\pi r_1^2} L_1^{(1)}(\theta, r_1, r_2, i) + X_0^{(1)} \left(L_0^{(1)}(\theta, r_1, r_2, i) - \frac{3}{2} L_1^{(1)}(\theta, r_1, r_2, i) \right),$$

$$L(\theta, r_1, r_2, i, X_0^{(1)}, X_1^{(1)}) \quad (22)$$
$$= \frac{2L^{full}}{\pi r_1^2} L_2^{(1)}(\theta, r_1, r_2, i) + X_0^{(1)} (L_0^{(1)}(\theta, r_1, r_2, i) - 2L_2^{(1)}(\theta, r_1, r_2, i)) + X_1^{(1)} (L_1^{(1)}(\theta, r_1, r_2, i) - \frac{4}{3} L_2^{(1)}(\theta, r_1, r_2, i)).$$

We can also exclude $I_0^{(1)}$ from (3) and (4) by expressing it using the right-hand sides of (7) and (8), respectively. This yields

$$X_0^{(1)} = \frac{3L^{full}(1 - x_1)}{\pi r_1^2 (3 - x_1)} \quad (23)$$

for the linear limb-darkening law and

$$X_0^{(1)} = \frac{6L^{full}(1 - x_1 - 2y_1)}{\pi r_1^2 (6 - 2x_1 - y_1)}, \quad (24)$$
$$X_1^{(1)} = \frac{6L^{full}(x_1 + 2y_1)}{\pi r_1^2 (6 - 2x_1 - y_1)}$$

for the quadratic limb-darkening law. The inverse expressions for (23) and (24) are

$$x_1 = \frac{6L^{full}}{\pi r_1^2 X_0^{(1)} - 3L^{full}} \quad (25)$$

and

$$x_1 = \frac{\pi r_1^2 (12X_0^{(1)} + 11X_1^{(1)}) - 12L^{full}}{3\pi r_1^2 (X_0^{(1)} + X_1^{(1)})}, \quad (26)$$
$$y_1 = \frac{6L^{full} - \pi r_1^2 (6X_0^{(1)} + 4X_1^{(1)})}{3\pi r_1^2 (X_0^{(1)} + X_1^{(1)})}.$$

When searching for the residual minima, we first minimize the residual functional in the linear parameters $X_0^{(1)}$ and $X_1^{(1)}$, since this linear minimization can be carried out analytically, yielding analytic expressions for the parameters $\widetilde{X_0^{(1)}}(r_1, r_2, i)$ and $\widetilde{X_1^{(1)}}(r_1, r_2, i)$ and their derivatives corresponding to the minimum residual for r_1, r_2, and i fixed. The character of the statistical distribution of the minimum residuals remains unchanged in the case of a linear minimization, and only the number of degrees of freedom changes (decreases) for this distribution. Further minimization is then performed for a nonlinear function of three variables: r_1, r_2, and i. The differential-correction method directly finds the central values of r_1, r_2, i, $X_0^{(1)}$, $X_1^{(1)}$, and their covariations. We then turn to the parameters r_1, r_2, i, x_1, and y_1 using (25) and (26). The dispersion estimates in the differential-correction method are derived in the same way as for the model obtained with the corresponding change of variables [12]. Note that a non-linear minimization changes the statistical distribution of the minimum residuals [10], so that it only asymptotically approaches the χ^2_M distribution (as $M \to \infty$). Since the number of data points in the HD 209458 light curves is large in our case ($M \gtrsim 500$), the minimization of the residuals between the observed and theoretical light curves should yield reliable asymptotic confidence regions for the fitted model parameters. We will designate

Table 1. Fitting of the observed light curve of HD 209458 from [1] using the linear limb-darkening law. The parameter uncertainties were estimated using the differential-correction and confidence-region methods assuming χ^2_P (where P is the number of parameters) and χ^2_M (where M is the number of data points in the light curve) statistics

Parameter	Differential-correction method (2σ)	Confidence-region method, χ^2_P (95%)	Confidence-region method, χ^2_M (95%)	Parameters from [5] (1σ)
$r_s, R_\odot$	0.11469 ± 0.000759	0.1147 ± 0.001186	0.1147 ± 0.00079	0.11482 ± 0.00035
$r_p, R_\odot$	0.014057 ± 0.0001149	0.01406 ± 0.0001808	0.01406 ± 0.0001211	0.014076 ± 0.000055
i, degrees	86.48 ± 0.083	86.48 ± 0.1318	86.48 ± 0.13	86.472 ± 0.038
x	0.49452 ± 0.009306	0.4944 ± 0.01406	0.4945 ± 0.00954	0.494 ± 0.004
χ^2_{red}		1.103		1.1457

the limb-darkening coefficients in the linear limb-darkening law x, without the subscript 1, while the linear and quadratic limb-darkening coefficients in the quadratic limb-darkening law will continue to be designated x_1 and y_1. In some cases, we denote the stellar radius r_1 and the planetary radius r_2 as r_s and r_p, to make the notation clearer.

3. OBSERVATIONAL MATERIAL

We analyze here precision transit light curves of the exoplanet binary HD 209458 from [1, 2] obtained with the Hubble Space Telescope (HST).

The observed light curve presented in [1] was obtained in April–May 2000. The spectra were obtained using the STIS spectrometer with the G750M spectral grating. The observations were performed at 5813–6382 Å with a resolution of $R = \lambda/\Delta\lambda = 5440$ (see [1] for more detail). The normalized light curve for the transit of the exoplanet across the stellar disk is displayed in Fig. 1. The light curve consists of 556 individual brightness measurements. The rms uncertainties for the individual measurements are between $\sigma_i^{obs} = 1.13 \times 10^{-4}$ and $\sigma_i^{obs} = 2.47 \times 10^{-4}$ (in units of the out-of-eclipse intensity) in different parts of the light curve. The relative uncertainties (expressed as fractions of the eclipse depth) are between $\sim 7 \times 10^{-3}$ and $\sim 1.5 \times 10^{-2}$.

HST data obtained between May 3 and July 6, 2003 are presented in [2]. The spectra were acquired using the STIS spectrometer with the G430L (2930–5670 Å) and G750L (5320–10 190 Å) spectral gratings. Applying two spectral gratings made it possible to cover a fairly wide wavelength range, from 2900 Å to 10 300 Å. For their further analysis, Knutson et al. [2] subdivided this wavelength range into ten equal parts, providing light curves in ten different photometric bands. The light curves for the central wavelengths 3201, 3750, 4300, 4849, and 5398 Å consist of 505 individual brightness measurements each; the light curves for the central wavelengths 5802, 6779, 7755, 8732, and 9708 Å consist of 548 individual measurements. The observed transit light curves from [2] are displayed in Fig. 2. The rms uncertainties of the individual measurements vary between $\sigma_i^{obs} = 1.79 \times 10^{-4}$ and $\sigma_i^{obs} = 6.09 \times 10^{-4}$ (or between $\sim 10^{-2}$ and $\sim 3 \times 10^{-2}$ in fractions of the eclipse depth). More detailed information on these observations and their reduction can be found in [2]. We assume that the observational errors obey a normal distribution and that systematic errors are negligible.

4. FITTING OF THE HD 209458 LIGHT CURVES FOR THE LINEAR LIMB-DARKENING LAW

The fitted parameters in our analysis of the observed light curves are the radius of the exoplanet r_p, the radius of the star r_s, the orbital inclination i, and the linear limb-darkening coefficient x. The orbital period adopted for the binary was $P_{orb} = 3.52474859^{\mathrm{d}}$ [2], the ratio of the masses of the planet and star was taken to be $q = m_p/m_s = 0.00055$ [2], the orbit of the system was assumed to be circular, and we adopted a unit radius for the relative orbit.

4.1. Light Curve from Brown et al. [1]

Table 1 presents the central values of the derived parameters and their uncertainties estimated using the differential-correction method (equivalent, as we noted above, to the Monte Carlo method [11, 12]) and the confidence-region method assuming χ^2_P (where P is the number of derived parameters) and χ^2_M (where M is the number of observed data points) statistics. We selected the $\gamma = 95\%$ confidence level, corresponding to 2σ in the differential-correction method, where σ is the standard deviation.

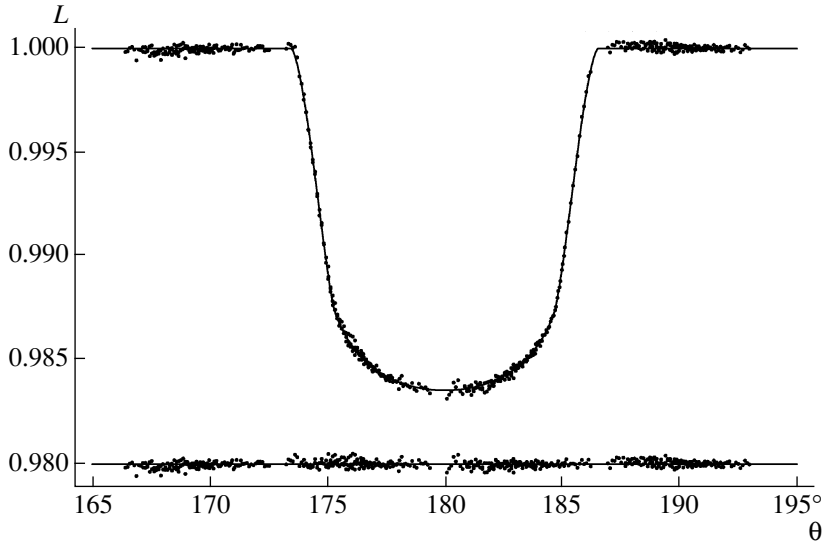

Fig. 1. Observed (points) and theoretical (solid curve) light curves for the binary with an exoplanet HD 209458 from [1]. In the bottom, we show the deviations of the observed brightness from the theoretical light curve calculated using the non-linear (quadratic) limb-darkening law.

Our test of the consistency between the model and observations demonstrated that the ratio of the minimum deviation to $M-P$ (distributed according to a reduced χ^2 law with $M-P$ degrees of freedom) is $\chi^2_{red} = \widetilde{\chi^2_{M-P}} \simeq 1.103$. Using the results from [12], we conclude that our model can be rejected at the $\alpha \gtrsim 0.05889$ significance level (this confidence level corresponds to a half-interval $\sim 1.889\sigma$). Thus, our model is rejected at a very low significance level ($\alpha = 6\%$); therefore, it is not very good, but also not hopelessly bad, since we can estimate the confidence intervals using a statistic distributed as χ^2_M at the confidence level $\gamma = 0.95$ in order to obtain the most conservative uncertainty estimates for the parameters. Note that, for this observed light curve, the uncertainty estimates in the confidence-region method obtained assuming χ^2_P statistics exceed those obtained assuming χ^2_M statistics. According to the formula for the distribution of the ratio of these intervals from [12] (assuming that the model is perfectly correct), the probability of this occurring is low: approximately 4%.

The fact that our model is not very good (in rejecting the model, we would be incorrect in less than ∼6% of cases and correct in more than ∼94% of cases) does not seem surprising. First, we used the linear limb-darkening law, which describes the brightness distribution across the stellar disk only roughly. In addition, our model does not take into account fine structure on the stellar disk: spots, plages, and active areas, whose sizes can be comparable to that of the eclipsing planet. We have also neglected possible intrinsic micro-variations of the star. These factors could cause short-time-scale irregularities of the star's brightness variations during its eclipse by the planet, exceeding the statistical uncertainty of the observations. Such irregularities are especially noticeable in the lower part of the light curve of Brown et al. (Fig. 1), where the brightness deviations from the light curve reach 5×10^{-4} mag (sometimes larger), appreciably in excess of the statistical uncertainty of the observations. It is precisely the fact that our model was found not to be very good that leads us to use the 95% rather than the 68% confidence level, as is usual in the case of "good" models. A suitable criterion of a "good" model is $\chi^2_{red} = \widetilde{\chi^2_{M-P}} \leq 1 + 2t$, where t is of the order of $\dfrac{P}{M}$ (it follows from this condition, that the model be acceptable at the $\gamma \to 50\%$ confidence level as $M \to \infty$).

Table 1 presents projections of the asymptotic confidence region D in the space of the four fitted parameters onto the axes of the parameters r_p, r_s, i, and x (the confidence intervals). The probability of such a projection of the confidence region D (confidence interval) emcompassing the true parameter value exceeds 95%. The probability that the exact solution is emcompassed by the asymptotic confidence region D is guaranteed to be close to the adopted probability of 95% (because the number of light-curve data points is high, $M > 500$). The probability that the exact solution will be encompassed by all the projections of the confidence region D (corresponding to the exact solution being in the parallelepiped of parameter space enclosing the confidence region D)

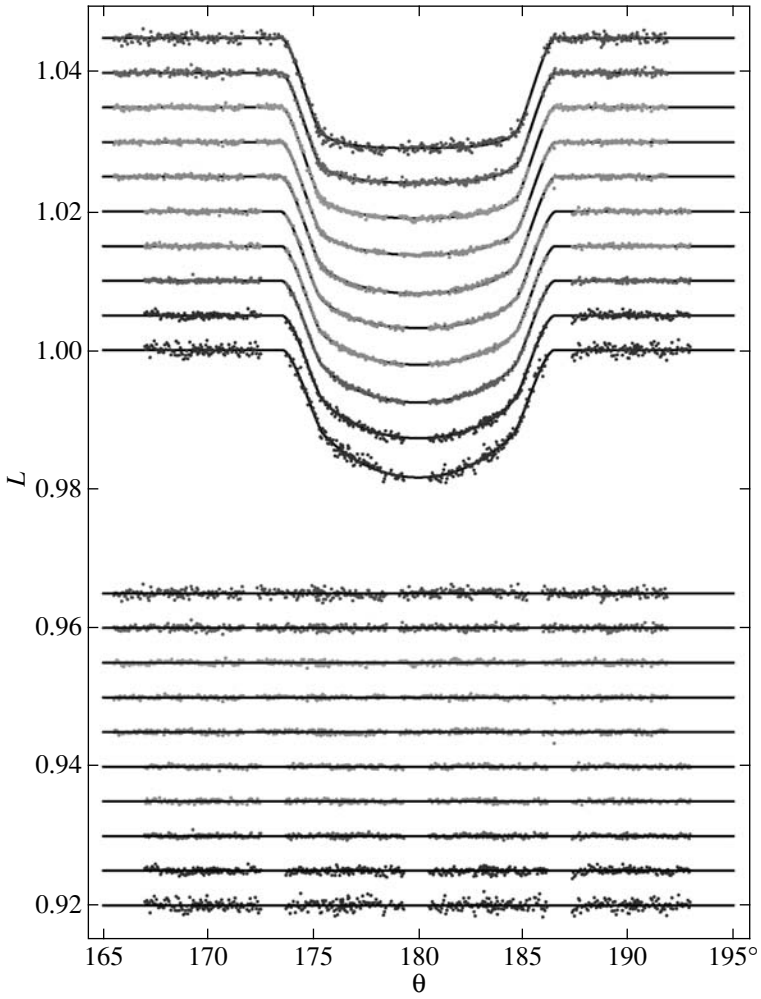

Fig. 2. The observed light curves of the exoplanet binary HD 209458 from [2] at 3201, 3750, 4300, 4849, 5398, 5802, 6779, 7755, 8732, and 9708 Å (from bottom to top). The corresponding distributions of the residuals are shown in the lower part of the panel. The solid curves are the theoretical light curves for the non-linear (quadratic) limb darkening.

is higher than the adopted probability, 95%. Note that all these statements concerning the probabilities of encompassing the exact solution have been strictly proven mathematically [13], and also confirmed with numerical modeling [11, 12]. Thus, adopting the projections of the confidence region D onto the parameter axes (confidence intervals) as the uncertainties of these parameters, we can definitely guarantee that the probability that the exact solution is encompassed by the confidence region D coincides with the adopted probability, 95%. This justifies our conservative uncertainty estimates for the fitted parameters as projections of the confidence region D onto the parameter axes (Table 1), which can be considered "external" errors of the fitted parameters r_p, r_s, i, and x.

Let us clarify the method used to find the projection of the confidence region D onto the parameter axes. To find the projection of the four-dimensional confidence region D onto the axis of some parameter—for example, r_p—we first minimize the deviation between the observed and theoretical light curves allowing all the parameters but the given one (i.e., r_p) to vary. The intersection of this curve with the straight line (critical level) corresponding to a given significance level α is then found (for the chosen statistics: χ^2_M, χ^2_P). The values of r_p providing deviations below the critical level when the minimization is carried out over all the remaining parameters (r_s, i, x) are combined into the confidence interval, which is just the projection of the four-dimensional confidence region D onto the r_p axis. This confidence interval encompasses the true value of r_p with a probability exceeding the adopted confidence level, $\gamma = 1 - \alpha$. Here, it is guaranteed that the exact solution (combining the true parameters r_p, r_s, i, x) is encompassed by the four-dimensional confidence region D with the adopted probability, $\gamma = 1 - \alpha$.

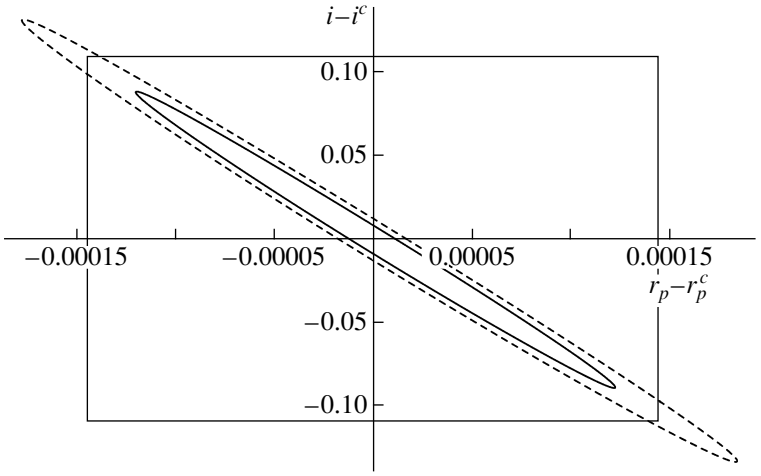

Fig. 3. The projection of the confidence region D (at the 95% confidence level) onto the (r_p, i) plane obtained for our fitting of the light curve from [1] using the linear limb-darkening law. The smaller ellipse (solid curve) corresponds to the confidence region found assuming χ^2_M statistics and the larger ellipse (dashed curve) to the confidence region found assuming χ^2_P statistics. The rectangle corresponds to the projection of the confidence region at the level $2\sigma_{est}$ found using the differential-correction method.

Figure 3 displays the projection of the confidence region D onto the r_p, i parameter plane. The projection characterizes the shape of the confidence region D. It is impossible to reproduce the whole multi-dimensional region D in a plane. The rectangle is the projection of the region defined by the parameter uncertainties (at the 2σ level) found using the differential-correction method. Because the linear limb-darkening fit to the precise light curve by Brown et al. [1] was rejected at a fairly low significance level (see above), the difference in the sizes of the projections of the confidence regions found using the differential-correction and confidence-region method is not large (however, see Figs. 11 and 12 below).

The probability of encompassing the true value of each of the parameters with the $\pm 2\sigma$ interval corresponds to the adopted probability, $\gamma = 95\%$. However, the probability to simultaneously encompass the true values with all the intervals found in the differential-correction method is lower than this probability (by approximately a factor of $\sim$1.5). Thus, the probability of the corresponding four-dimensional uncertainty region simultaneously encompassing all the fitted parameters is appreciably reduced if we adopt the "internal" parameter errors found in the differential-correction method or Monte Carlo method under the assumption that the model is perfectly correct (see also Figs. 11 and 12 below). This can explain why the results of fitting observations acquired on different epochs often disagree beyond the "internal" errors and the parameter uncertainties derived in the differential-correction (or Monte Carlo) method are often unrealistically small.

4.2. Multi-Color Light Curves of Knutson et al. [2]

The light curves for HD 209458 obtained in [2] at $\lambda = 3201$, 3750, 4300, 4849, 5398, 5802, 6779, 7755, 8732, and 9708 Å are presented in Fig. 2 (the wavelength λ increases from bottom to top). Tables 2–4 present the results of fitting these light curves using various methods to estimate the uncertainties of the fitted parameters: the confidence-region method assuming χ^2_M statistics (Table 2; dashes correspond to the degeneration of the "exact" confidence region into an empty set because the model is rejected at the adopted significance level, $\alpha = 5\%$) and χ^2_P statistics (Table 3) and the differential-correction method (Table 4; assuming a normal distribution for the resulting central values of the fitted parameters and that the model is perfectly correct). The χ^2_{red} value for the $\lambda = 5802$ Å light curve is especially large ($\chi^2_{red} = 1.299$; the model is rejected at a very low significance level: $\alpha = 5.168 \times 10^{-6}$). This light curve was probably influenced by some additional sources of error. The χ^2_{red} values for the other wavelengths are within reasonable limits: $\chi^2_{red} = 1.021$–1.122.

Our test for consistency between the model and observations demonstrates that the minimum deviation for the reduced χ^2 statistics exceeds unity (Table 3).

Using the χ^2_M statistics in the fitting of the light curves at $\lambda = 3201$, 3750, 4849, 5398, 6779, 7755, 8732 Å demonstrates that our model is not rejected at the $\alpha = 5\%$ significance level (and can be accepted). In all these cases, it is possible to derive "exact" confidence regions D (i.e., encompassing the true

Table 2. Results of fitting the observed multi-color light curves of HD 209458 from [2] using the linear limb-darkening law. The parameter uncertainties were found using the confidence-region method and χ^2_M statistics; $\gamma = 0.95$

λ, Å	r_s	$\Delta_M(r_s)$	r_p	$\Delta_M(r_p)$	i	$\Delta_M(i)$	x	$\Delta_M(x)$
3201	0.112422	0.00909003	0.0136815	0.00168653	87.0418°	1.25441°	0.839899	0.112573
3750	0.111096	0.00518492	0.0135058	0.000908670	87.0084	0.685166	0.755113	0.0601379
4300	0.113224	–	0.0138670	–	86.9607	–	0.702653	–
4849	0.113315	0.00215386	0.0138638	0.000353872	86.6501	0.257024	0.617381	0.0267281
5398	0.114474	0.00332352	0.0140443	0.000534038	86.5317	0.387603	0.561101	0.0420762
5802	0.114536	–	0.0141229	–	86.4712	–	0.534661	–
6779	0.115384	0.00210354	0.0141542	0.000327598	86.3841	0.240432	0.436149	0.0332838
7755	0.114060	0.00232615	0.0139412	0.000348055	86.5030	0.266790	0.377645	0.0363709
8732	0.115301	0.00451503	0.0141478	0.000672640	86.3800	0.515776	0.317885	0.0829246
9708	0.114814	–	0.0141637	–	86.3856	–	0.276457	–

Table 3. Results of fitting the observed multi-color light curves of HD 209458 from [2] using the linear limb-darkening law. The parameter uncertainties were found using the confidence-region method and χ^2_P statistics; $\gamma = 0.95$ (the last column contains the reduced χ^2_{red} and the corresponding significance level α)

λ, Å	r_s	$\Delta_P(r_s)$	r_p	$\Delta_P(r_p)$	i	$\Delta_P(i)$	x	$\Delta_P(x)$	$\frac{\chi^2_{M-P}}{M-P}$ (α)
3201	0.112789	0.00564078	0.0137580	0.00103572	86.8383°	0.721357°	0.833506	0.0703594	1.103 (0.069)
3750	0.111132	0.00318612	0.0135114	0.000556307	86.9630	0.412798	0.754423	0.0371808	1.067 (0.174)
4300	0.113232	0.00197803	0.0138682	0.000343468	86.6565	0.241463	0.702492	0.0233387	1.121 (0.041)
4849	0.113315	0.00162566	0.0138639	0.000267189	86.6468	0.193893	0.617462	0.0201586	1.084 (0.118)
5398	0.114449	0.00171209	0.0140408	0.000274972	86.5227	0.198908	0.561665	0.0217482	1.046 (0.271)
5802	0.114557	0.00138946	0.0141275	0.000228711	86.4703	0.162999	0.533942	0.0205499	1.299 (5.168×10^{-6})
6779	0.115386	0.00125488	0.0141545	0.000195295	86.3806	0.143095	0.436699	0.0198472	1.061 (0.186)
7755	0.114069	0.00158054	0.0139423	0.000236676	86.4989	0.181210	0.378139	0.0247354	1.0739 (0.138)
8732	0.115295	0.00199596	0.0141482	0.000297907	86.3629	0.226904	0.323146	0.0361643	1.021 (0.403)
9708	0.114743	0.00268813	0.0141555	0.000389998	86.4012	0.301402	0.275733	0.0483915	1.122 (0.0334)

values with the adopted probability, $\gamma = 95\%$) and to find projections of the region D onto the r_p, r_s, i, and x parameter axes (confidence intervals), which represent the most conservative, "external" uncertainties of the parameters (Table 2). Our model is rejected at the $\alpha < 5\%$ significance level (is "bad") for three light curves ($\lambda = 4300$, 5802, 9708 Å). For these light curves, we are able to find only the external uncertainties of the parameters (confidence intervals) for the χ^2_P statistics, corresponding to the asymptotic confidence region D, as well as the internal uncertainties of the parameters assuming normal statistics for the derived central parameter values using the differential-correction method. However, as is noted in [10], we should not forget that, in practice, we are dealing not with a complete observed random function (light curve) but a particular observational realization of this function. Thus, it is possible that the encountered difficulties with the fitting (the model is rejected at a rather low significance level, so that the confidence region D for the χ^2_M statistics degenerates into an empty set) are due to chance fluctuations of the observed function rather than flaws in the model. The applied model could be quite satisfactory for a different observational realization of the observed function, for example, for a light curve obtained at a

Table 4. Results of fitting the observed multi-color light curves of HD 209458 from [2] for the linear limb-darkening law. The parameter uncertainties were found using the differential-correction method; the 2σ uncertainties are given

λ, Å	r_s^c	$2\sigma_{est}\,(r_s^c)$	r_p^c	$2\sigma_{est}\,(r_2^c)$	i^c	$2\sigma_{est}\,(i^c)$	x^c	$2\sigma_{est}\,(x^c)$
3201	0.113113	0.00424010	0.0138328	0.000794048	86.7178°	0.537230°	0.828541	0.0505626
3750	0.111175	0.00224100	0.0135199	0.000396390	86.9333	0.292384	0.753992	0.025672
4300	0.113224	0.00127895	0.0138670	0.000220652	86.6507	0.154521	0.702653	0.0153839
4849	0.113302	0.00107659	0.0138618	0.000176852	86.6440	0.1282050	0.617614	0.0134061
5398	0.114456	0.00107583	0.0140421	0.000172042	86.5177	0.1239884	0.561705	0.0140619
5802	0.114535	0.00093831	0.0141229	0.000154114	86.4712	0.1097888	0.534661	0.0144226
6779	0.115394	0.00076714	0.0141560	0.000118926	86.3777	0.0869080	0.436943	0.0125312
7755	0.114035	0.00098878	0.0139372	0.000146933	86.4998	0.1119664	0.379030	0.0157685
8732	0.115326	0.00120960	0.0141535	0.000179209	86.3547	0.1355734	0.323969	0.0223688
9708	0.114814	0.00185497	0.0141637	0.000267488	86.3856	0.2046620	0.276457	0.0342494

different epoch, for which it would be rejected at a high significance level, enabling derivation of the confidence region D for the χ^2_M statistics. This suggests it could be meaningful to search for the asymptotic confidence region for the χ^2_P statistics (which, by definition, never degenerates into an empty set), even when the model is rejected at a fairly low significance level and is "bad."

It is interesting to compare the geometrical parameters of the HD 209458 system derived for different epochs. Table 5 presents the parameters for the $\lambda\lambda(5813-6382)$ Å light curve obtained by Brown et al. [1] in April–May 2000 and the light curve with the central wavelength $\lambda 6779$ Å ($\Delta\lambda = 6279-7279$ Å) obtained by Knutson et al. [2] in May–July 2003 together with their uncertainties. The half-intervals for the largest differences in the central parameter values are $\frac{|r_p^{(2000)} - r_p^{(2003)}|}{2} = 0.00004775°$, $\frac{|r_s^{(2000)} - r_s^{(2003)}|}{2} = 0.00034050°$, $\frac{|i^{(2000)} - i^{(2003)}|}{2} = 0.0515°$. These differences are within the internal 2σ uncertainties and certainly within the Δ_M and Δ_P confidence intervals (Table 5).

It is also of interest to compare the geometrical parameters (r_p, r_s, i) for the light curves of HD 209458 obtained by Knutson et al. [2] for the same epoch (May–July 2003) but at different wavelengths. The results of this comparison are collected in Table 6. The values of r_p, r_s, and i derived for different wavelengths do not quite agree within the internal 2σ uncertainties. At the same time, these geometrical parameters are in good agreement within the external Δ_P uncertainties, and especially the Δ_M uncertainties.

5. WAVELENGTH DEPENDENCE OF THE LINEAR LIMB-DARKENING COEFFICIENT

Since a simple model with linear limb-darkening applied to the light curves of Brown et al. [1] and Knutson et al. [2] is not hopelessly "bad" and is rejected only at a significance level α of several percent (except for the $\lambda = 5802$ Å light curve), it is reasonable to analyze the dependence of the limb-darkening coefficient x in the linear limb-darkening law on the wavelength λ and compare this dependence to the corresponding theoretical relation that follows from the theory of thin stellar atmospheres.

Table 7 presents our values for x and their uncertainties (2σ, Δ_P, Δ_M) as functions of λ. We minimized the residual functional for each λ in four parameters: r_p, r_s, i, x. The dashes correspond to cases when the model is rejected at the significance level $\alpha < 5\%$. Table 7 shows that, with the most conservative estimates of the external uncertainties in x (for the χ^2_M statistics), the relative uncertainties in x are 8%–13% in the blue ($\lambda = 3201-3750$ Å), 4%–8% in the visible ($\lambda = 4849-6779$ Å), and 8%–26% in the red ($\lambda = 7755-8732$ Å).

The dependence of the linear coefficient x (in the linear limb-darkening law) on the wavelength λ is presented in Figs. 4 and 5. We used the results of Claret [15] for the $ugriz$ and $UBVRIJ$ photometric systems for the theoretical wavelength dependence of x. Using different photometric systems indicates the extent to which the $x(\lambda)$ relation is determined by the choice of photometric system (the need for such a check was emphasized in [5]).

Table 5. Differences between geometrical parameters derived from light curves for different epochs: internal and external uncertainties

Largest parameter differences	Differences in central parameter values	Differential-correction method (2σ)	Confidence-region method, χ^2_P (95%)	Confidence-region method, χ^2_M (95%)
$\frac{\lvert r_p^{(2000)} - r_p^{(2003)}\rvert}{2}$	0.000048	0.00012	0.00018	0.00033
$\frac{\lvert r_s^{(2000)} - r_s^{(2003)}\rvert}{2}$	0.00034	0.00077	0.0012	0.0021
$\frac{\lvert i^{(2000)} - i^{(2003)}\rvert}{2}$	0.051°	0.087°	0.13°	0.24°

Table 6. Scatter of the derived central values of the fitted geometrical parameters found from 10 light curves for various wavelengths (the ratios of the (max−min)/2 semi-interval to the corresponding mean values of the uncertainty intervals from Tables 2, 3, 4 are given in brackets)

Parameter	Largest scatter of the central values (min−max)	Differential-correction method (2σ)	Confidence-region method, χ^2_P (95%)	Confidence-region method, χ^2_M (95%)
r_s	0.111096–0.115394	0.112373–0.115507 (1.37)	0.112076–0.115984 (1.10)	0.109620–0.117820 (0.52)
r_p	0.0135058–0.0141542	0.0137074–0.0142326 (1.23)	0.013667–0.014293 (1.04)	0.013220–0.014600 (0.47)
$k = r_p/r_s$	0.121609–0.123362	0.121876–0.123264 (1.26)	0.12157–0.12357 (0.88)	0.12077–0.124219 (0.47)
i, degrees	86.3547–87.0400	86.36–86.74 (1.82)	86.31–86.77 (1.49)	86.13–87.15 (0.67)

Table 7. Limb-darkening coefficients derived for the linear limb-darkening law. The central values and indicated 2σ uncertainty intervals were found using the differential-correction method and the confidence-region method assuming χ^2_P and χ^2_M statistics ($\gamma = 0.95$)

λ, Å	x^c	$2\sigma_{est}(x^c)$	x	$\Delta_P(x)$	x	$\Delta_M(x)$
3201	0.828541	0.0505626	0.833506	0.0703594	0.839899	0.112573
3750	0.753992	0.0256720	0.754423	0.0371808	0.755113	0.0601379
4300	0.702653	0.0153839	0.702492	0.0233387	–	–
4849	0.617614	0.0134061	0.617462	0.0201586	0.617381	0.0267281
5398	0.561705	0.0140619	0.561665	0.0217482	0.561101	0.0420762
5802	0.534661	0.0144226	0.533942	0.0205499	–	–
6779	0.436943	0.0125312	0.436699	0.0198472	0.436149	0.0332838
7755	0.379030	0.0157685	0.378139	0.0247354	0.377645	0.0363709
8732	0.323969	0.0223688	0.323146	0.0361643	0.317885	0.0829246
9708	0.276457	0.0340324	0.275733	0.0483915	–	–

Figure 4 shows the central values of x derived using the differential-correction method together with their internal 2σ uncertainties. In general, our results are in good agreement with those of Southworth [5]. Figure 4 shows that the linear limb-darkening coefficients x derived from the observed light curves do not agree with the theoretical values.

Figure 5 displays the central values of x and the most conservative estimates of the external uncertainties obtained using the confidence-region method and χ^2_M statistics. Note that we adopted $\gamma = 95\%$.

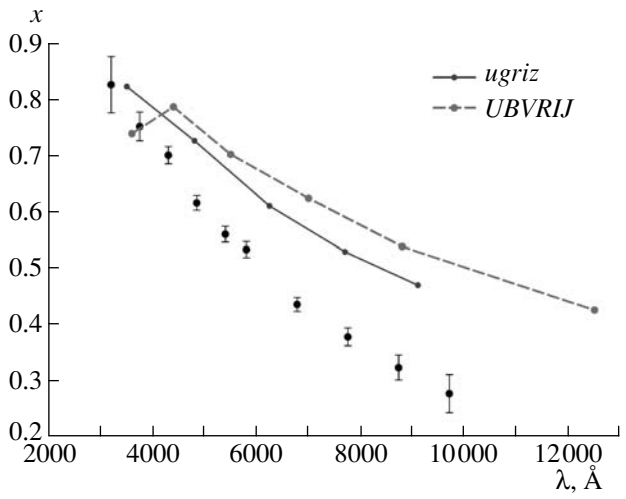

Fig. 4. Wavelength dependence of the limb-darkening coefficient x for HD 209458 for the linear limb-darkening law. The limb-darkening coefficients were derived from the light curves of [2]. The quoted 2σ uncertainties in the limb-darkening coefficients were determined using the differential-correction method. The theoretical limb-darkening coefficients in the $ugriz$ and $UBVRIJ$ photometric systems are plotted according to [15].

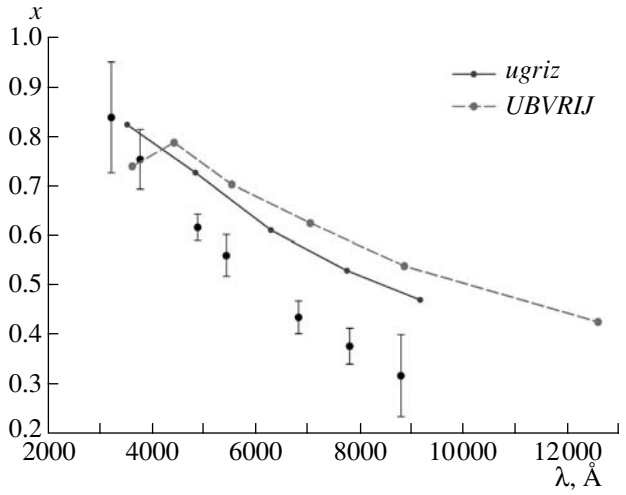

Fig. 5. Same as Fig. 4 for the uncertainties in the limb-darkening coefficients derived using the confidence-region method assuming χ^2_M statistics; the confidence level is $\gamma = 0.95$.

This figure also shows the corresponding theoretical $x(\lambda)$ relations of Claret [15]. Although the uncertainties in x increased by a factor of two to four compared to the internal 2σ uncertainties, the discrepancy between the observed and theoretical limb-darkening coefficients, $x(\lambda)$, remains significant. The observed $x(\lambda)$ values are systematically below the theoretical ones, with the difference increasing with wavelength. This result is very important for improving current models of thin stellar atmospheres.

Tables 2–4 contain the $x(\lambda)$ values and their uncertainties obtained by minimizing the residuals between the observed and theoretical light curves in the four parameters r_p, r_s, i, and x. In this case, each x value for a given wavelength λ corresponds to its own set of the geometrical parameters r_p, r_s, and i. At the same time, it is clear that i should not depend on λ. The planet's radius may depend on λ because it has an atmosphere, but this effect is small and can be detected only in very precise eclipse light curves (for instance, cf. [16]). Therefore, we determined the limb-darkening coefficients $x(\lambda)$ for the fixed geometrical parameters r_p, r_s, and i, common for all λ. We adopted the arithmetic means of all the values of r_p, r_s, i found for the different λ for these fixed values: $\overline{r}_p = 0.0139657$, $\overline{r}_s = 0.113937$, $\overline{i} = 86.55°$.

The limb-darkening coefficients $x(\lambda)$ and their uncertainties derived via minimization of the residuals with fixed $\overline{r}_p$, $\overline{r}_s$, and $\overline{i}$ are collected in Table 8. We believe that these $x(\lambda)$ values are the most reliable representation of the wavelength dependence of x, shown in Fig. 6. The presented external uncertainties are the Δ_P values found assuming χ^2_P statistics. When χ^2_M statistics are used, the model is rejected at the $\alpha < 5\%$ significance level in most cases, because the more rigid model assumption that the geometrical parameters are the same for all wavelengths are applied in this case. This model can be accepted at the level $\alpha = 5\%$ for only three wavelengths ($\lambda\lambda$4849, 5398, 8732 Å). Table 8 presents the corresponding central values, $x(\lambda)$, and the most conservative estimates of the external uncertainties obtained assuming χ^2_M statistics.

6. INTERPRETATION OF THE HD 209458 LIGHT CURVES USING THE QUADRATIC LIMB-DARKENING LAW

Southworth [5] also presents the quadratic limb-darkening coefficients derived from the multi-color light curves of HD 209458 [2]. Southworth [5] notes that the linear limb-darkening model can be rejected for the most accurate light curve obtained by Brown et al. [1], at a high significance level (exceeding 99.99%). This conclusion qualitatively agrees with our own results (see above), but there remain quantitative differences. Usually, the significance level α of a statistical test (see, for example, [13]) is understood as the number of errors of the first kind we make when applying the test. An error of the first kind is a situation when a correct model is rejected by the statistical test. According to [5], if the model can be rejected at a significance level exceeding 99.99%, this means that,

Table 8. Results of fitting the observed light curves of HD 209458 from [2] using the linear limb-darkening law, fixing $\overline{r}_p$, $\overline{r}_s$, and $\overline{i}$ to be their averages for all wavelengths. The parameter uncertainties for $\gamma = 0.95$ were found using the confidence-region method and χ^2_P and χ^2_M statistics

λ, Å	x	$\Delta_P(x)$	x	$\Delta_M(x)$	χ^2_{red}
3201	0.805194	0.0196023	–	–	1.127
3750	0.732868	0.0117864	–	–	1.208
4300	0.697317	0.00718819	–	–	1.190
4849	0.608848	0.00705112	0.608828	0.00992982	1.103
5398	0.552146	0.00778080	0.552016	0.0194529	1.068
5802	0.552724	0.00662294	–	–	1.420
6779	0.445318	0.00680517	–	–	1.214
7755	0.395653	0.00922067	–	–	1.354
8732	0.352846	0.0125393	0.352893	0.00567959	1.110
9708	0.329928	0.0181280	–	–	1.158

when rejecting the model, we make an error of the first kind (reject the correct model) in 9999 cases of 10 000; i.e., we are correct in rejecting the model in only one case out of 10 000. Thus, we have no reason to reject the model in this case, and it can be accepted. When quoting the value 99.99%, Southworth [5] probably meant the confidence level $\gamma = 1 - \alpha$ rather than the significance level α. Correcting for this confusion, the linear limb-darkening model applied to the precise light curve of Brown et al. [1] is rejected in [5] at a very low significance level, $\alpha < 0.01\%$. Note that, according to [5], the minimum residual for the reduced χ^2 for the linear limb-darkening law (and the light curve of Brown et al. [1]) is $\chi^2_{red} = 1.1457$, corresponding, as follows from [12], to rejecting the model at the level $\alpha = 1\%$ (not $\alpha < 0.01\%$, as in [5]). According to our fitting, the linear limb-darkening model applied to the precise light curve of Brown et al. [1] is rejected at a low significance level ($\alpha \sim 6\%$), in agreement with the minimum reduced χ^2 value, $\chi^2_{red} = \chi^2_{M-P}/(M-P) \simeq 1.103$ [12]. Thus, as is noted above, the linear limb-darkening model is not very good, but also not hopelessly poor, since, in this case, we are able to estimate conservative parameter uncertainties at the $\gamma = 95\%$ confidence level.

We also fitted the precise light curve of Brown et al. [1] using the quadratic limb-darkening law. We minimized the residual functional in the five parameters r_p, r_s, i, x_1, and y_1, where x_1, y_1 are the coefficients in the limb-darkening law:

$$I(\mu) = I_0\left(1 - x_1(1-\mu) - y_1(1-\mu)^2\right).$$

Here, $\mu = \cos\omega$ (ω is the angle between the normal to the stellar surface and the line of sight). The results are presented in Table 9, which contains the central values of the parameters r_p, r_s, i, x_1, and y_1 and their uncertainties Δ found using the differential-corrections and confidence-region methods for $\gamma = 95\%$. The reduced χ^2 is also given ($\chi^2_{red} = 1.01340$), and is much lower than the reduced χ^2 for the linear limb-darkening model ($\chi^2_{red} = 1.103$). Our quadratic limb-darkening model is rejected at the significance

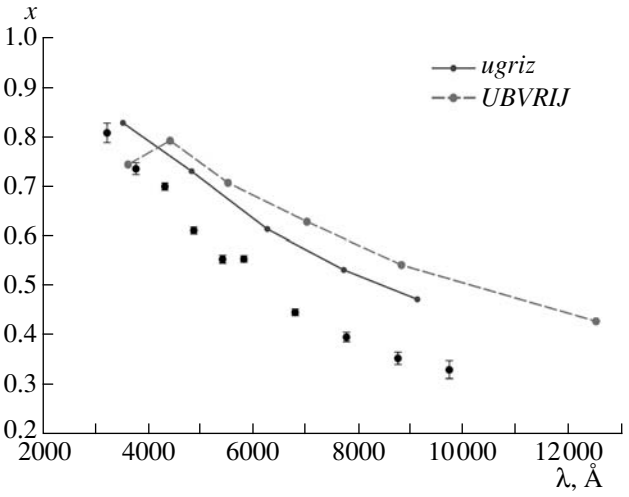

Fig. 6. Same as Fig. 5 for fixed $\overline{r}_p = 0.0139657$, $\overline{r}_s = 0.113937$, and $\overline{i} = 86^\circ.555243$, equal to their average values for all wavelength, and assuming χ^2_P statistics.

Table 9. Results of fitting the observed light curves of HD 209458 from [1] using the non-linear (quadratic) limb-darkening law. The parameter uncertainties were found using the differential-correction method and confidence-region method, assuming χ^2_P (P is the number of fitted parameters) and χ^2_M (M is the number of data points in the light curve) statistics. The bottom line contains the reduced χ^2_{red} values

Parameter	Differential-correction method (2σ)	Confidence-region method, χ^2_P (95%)	Confidence-region method, χ^2_M (95%)
r_1	0.113836	0.113845	0.113776
$\Delta(r_1)$	0.000853921	0.00145205	0.00324496
r_2	0.0137654	0.0137679	0.0137456
$\Delta(r_2)$	0.000144763	0.000250444	0.000562880
i^c, deg	86.6756	86.6789	86.7196
$\Delta(i)$, deg	0.108695	0.189625	0.429125
x_1	0.294517	0.296029	0.297905
$\Delta(x_1)$	0.0546122	0.0927646	0.207913
y_1	0.344130	0.343221	0.352285
$\Delta(y_1)$	0.0955230	0.163519	0.366437
χ^2_{red}	1.01340		

Table 10. Results of fitting the observed light curves of HD 209458 from [1] using the non-linear (quadratic) limb-darkening law. The parameter uncertainties were found using the differential-correction method and confidence-region method, assuming χ^2_P (P is the number of fitted parameters) and χ^2_M (M is the number of data points in the light curve) statistics. The chosen confidence level is $\gamma = 0.68$

Parameter	Differential-correction method (σ)	Confidence-region method, χ^2_P (68%)	Confidence-region method, χ^2_M (68%)
r_1	0.113836	0.113840	0.113844
$\Delta(r_1)$	0.000426960	0.00104013	0.00155419
r_2	0.0137654	0.0137677	0.0137676
$\Delta(r_2)$	0.0000723814	0.000179204	0.000268077
i, deg	86.6756	86.6765	86.6799
$\Delta(i)$, deg	0.0543473	0.135610	0.203029
x_1	0.294517	0.295082	0.296223
$\Delta(x_1)$	0.0273061	0.0662467	0.0993592
y_1	0.344130	0.343627	0.343281
$\Delta(y_1)$	0.0477615	0.116747	0.175127

level $\alpha > 46\%$, so that we are able to estimate the external parameter uncertainties at the $\sim$95% confidence level for both χ^2_P and χ^2_M statistics. Thus, the model with the quadratic limb-darkening law is "good" when applied to the precise light curve of Brown et al. [1] (in rejecting the model, we would make an error of the first kind, i.e. reject the correct model, in less than 46% of all cases). This indicates

Table 11. Results of fitting the observed light curves of HD 209458 from [2] using the non-linear (quadratic) limb-darkening law. The 2σ parameter uncertainties were found using the differential-correction method (the last two columns contain the reduced χ^2 values and the corresponding significance levels α)

λ, Å	r_1^c	$2\sigma_{\rm est}\,(r_1^c)$	r_2^c	$2\sigma_{\rm est}\,(r_2^c)$	i^c	$2\sigma_{est}\,(i^c)$	x_1^c	$2\sigma_{est}\,(x_1^c)$	y_1^c	$2\sigma_{est}\,(y_1^c)$	χ^2_{red}	α
3201	0.1128	0.003574	0.01407	0.0007801	86.59°	0.46°	1.024	0.1965	−0.3706	0.3530	1.062	0.205
3750	0.1113	0.002223	0.01360	0.0004571	86.88	0.31	0.7978	0.1074	−0.08720	0.2086	1.068	0.181
4300	0.1133	0.001312	0.01388	0.0002658	86.64	0.18	0.7105	0.07557	−0.01514	0.1408	1.123	0.0409
4849	0.1133	0.001122	0.01385	0.0002147	86.65	0.15	0.6119	0.07144	0.01035	0.1274	1.086	0.118
5398	0.1138	0.001222	0.01381	0.0002279	86.67	0.16	0.4286	0.07723	0.2419	0.1426	1.023	0.410
5802	0.1142	0.001034	0.01400	0.0001969	86.55	0.14	0.4551	0.08225	0.1389	0.1418	1.293	8.55×10^{-6}
6779	0.1149	0.0008532	0.01399	0.0001520	86.49	0.11	0.3066	0.07529	0.2183	0.1250	1.042	0.292
7755	0.1134	0.001130	0.01374	0.0001909	86.64	0.15	0.2035	0.09479	0.2899	0.1580	1.048	0.257
8732	0.1144	0.001424	0.01388	0.0002411	86.54	0.19	0.07225	0.1369	0.4119	0.2265	0.9966	0.574
9708	0.1136	0.002296	0.01380	0.0003744	86.64	0.30	−0.07901	0.2096	0.5815	0.3519	1.100	0.0702

Table 12. Results of fitting the observed light curves of HD 209458 from [2] usingr the quadratic limb-darkening law. The parameter uncertainties were found using the confidence-region method assuming χ^2_P statistics; the adopted confidence level is 95%

λ, Å	r_1	$\Delta_p\,(r_1)$	r_2	$\Delta_p\,(r_2)$	i	$\Delta_p\,(i)$	x_1	$\Delta_p\,(x_1)$	y_1	$\Delta_p\,(y_1)$
3201	0.1128	0.0053	0.01439	0.00140	86.53°	0.81°	1.04	0.30	−0.52	0.67
3750	0.1112	0.0034	0.01359	0.00068	86.93	0.49	0.80	0.16	−0.07	0.32
4300	0.1133	0.0023	0.01388	0.00051	86.66	0.34	0.72	0.13	−0.02	0.26
4849	0.1133	0.0018	0.01385	0.00035	86.66	0.25	0.62	0.12	0.01	0.21
5398	0.1138	0.0021	0.01380	0.00039	86.69	0.29	0.43	0.13	0.25	0.24
5802	0.1142	0.0016	0.01402	0.00031	86.55	0.22	0.46	0.13	0.13	0.22
6779	0.1149	0.0014	0.01399	0.00026	86.49	0.19	0.31	0.13	0.22	0.21
7755	0.1134	0.0018	0.01374	0.00030	86.64	0.24	0.21	0.15	0.29	0.25
8732	0.1144	0.0023	0.01388	0.00039	86.56	0.31	0.07	0.22	0.42	0.37
9708	0.1133	0.0038	0.01374	0.00063	86.73	0.53	−0.08	0.34	0.60	0.57

that the non-linear (quadratic) limb-darkening law is preferable to the linear law. Moreover, the quadratic limb-darkening model is sufficiently good that we can estimate the conservative external uncertainties of x_1 and y_1 at the $\gamma = 1 - \alpha = 68\%$ confidence level, collected in Table 10.

Our conservative estimate of the external uncertainties of the parameters x_1, y_1 at the 95% confidence level shows that the derived values of x_1, y_1 are at the detection limit (Table 9; see also Table 13). If we use only the internal uncertainties in x_1 and y_1 (Table 9) or the conservative external uncertainties at the 68%

Table 13. Results of fitting the observed light curves of HD 209458 from [2] using the quadratic limb-darkening law. The parameter uncertainties were found using the confidence-region method assuming χ^2_M statistics; the adopted confidence level is 95%

λ, Å	r_1	$\Delta_M(r_1)$	r_2	$\Delta_M(r_2)$	i	$\Delta_M(i)$	x_1	$\Delta_M(x_1)$	y_1	$\Delta_M(y_1)$
3201	0.1174	0.0141	0.01428	0.00249	86.96°	1.61°	0.91	0.43	−0.19	1.40
3750	0.1109	0.0051	0.01356	0.00110	87.01	0.81	0.81	0.26	−0.08	0.50
4300	–	–	–	–	–	–	–	–	–	–
4849	0.1133	0.0022	0.01385	0.00043	86.67	0.30	0.62	0.14	0.01	0.25
5398	0.1136	0.0044	0.01373	0.00085	86.79	0.65	0.42	0.26	0.28	0.52
5802	–	–	–	–	–	–	–	–	–	–
6779	0.1148	0.0027	0.01399	0.00050	86.51	0.36	0.32	0.24	0.21	0.40
7755	0.1133	0.0033	0.01373	0.00056	86.67	0.44	0.21	0.28	0.29	0.46
8732	0.1136	0.0056	0.01380	0.00105	86.72	0.86	0.09	0.58	0.44	0.95
9708	0.1134	0.0031	0.01376	0.00051	86.70	0.42	−0.08	0.28	0.60	0.47

confidence level (Table 10), we may consider the derived limb-darkening coefficients x_1, y_1 to correspond to their real values.

We also applied a model with a quadratic limb-darkening law to the multi-color light curves of Knutson et al. [2]. The corresponding fitting results are presented in Tables 11–13. It follows from Table 11 that, on average, χ^2_{red} is lower than for the model with the linear limb-darkening law (Table 3). Figures 7–10 display the coefficients x_1, y_1 as functions of the wavelength λ. We also show the theoretical x_1, y_1 values from Claret [15]. The non-linear coefficient y_1 for HD 209458 agrees with the theoretical relation within the errors. However, the observed values of the linear coefficient x_1 for the quadratic limb-darkening law significantly deviate from the theoretical values (as for the linear limb-darkening law). We show the projections of the confidence region D onto the x_1, y_1 and r_s, r_p parameter planes in Figs. 11 and 12. Here, the rectangles show the projections of the region defined by the 2σ parameter uncertainties found using the differential-correction method.

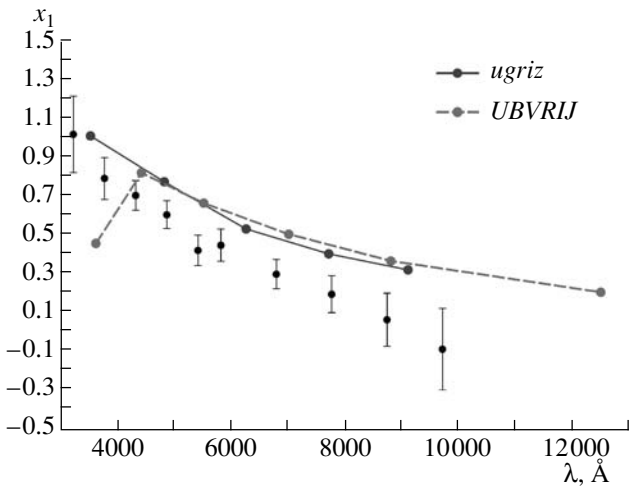

Fig. 7. Wavelength dependence of the limb-darkening coefficient x_1 for HD 209458 in the quadratic limb-darkening law. The limb-darkening coefficients were derived using the light curves of [2]. The quoted 2σ uncertainties in the limb-darkening coefficients were derived using the differential-correction method. The theoretical limb-darkening coefficients in the $ugriz$ and $UBVRIJ$ photometric systems are plotted according to [15].

7. USING THE APPROXIMATE METHOD SUGGESTED IN [12] TO ESTIMATE THE EXTERNAL PARAMETER UNCERTAINTIES

The above estimates of the external uncertainties for the parameters of the system HD 209458 were made via an exhaustive parameter search to find the corresponding surface of the residual functional in the multi-dimensional parameter space. The procedure used for the exhaustive parameter search is laborious, though it can be performed comparatively easily for our simple model (two spherical stars in a circular orbit). However, for other, more complex models the exhaustive parameter search can become difficult. Thus, we suggest in [12] an approximate method for estimating the external parameter uncertainties, which can easily be implemented practically. We present in [12] tables and corresponding

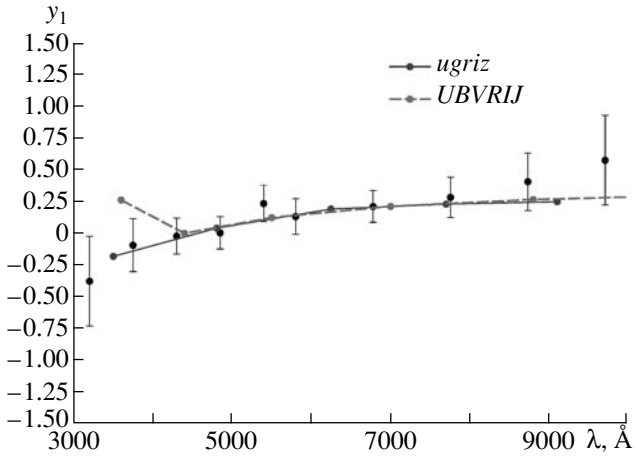

Fig. 8. Same as Fig. 7 for the limb-darkening coefficient y_1.

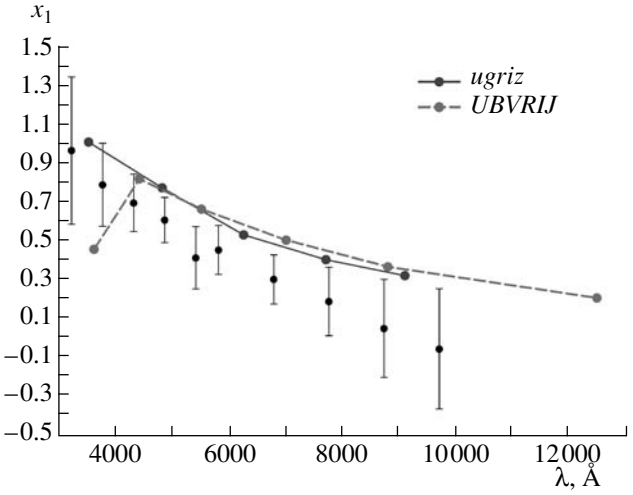

Fig. 9. Same as Fig. 7 for the case when the uncertainties in the limb-darkening coefficients are found using the confidence-region method with χ^2_P statistics; the confidence level is $\gamma = 0.95$.

diagrams that can be used to compute the coefficient for translation from the internal parameter uncertainties derived in the Monte Carlo or differential-correction method to the external uncertainties derived in the confidence-region method for χ^2_M statistics ($t_{\max}$ for the one-dimensional problem or $k_p t_{p\max}$ for the multi-dimensional problem) [12]. Having calculated the internal uncertainties $\delta_1(\gamma)$ and become convinced that the model used is consistent with the observations (for which it is sufficient to determine the minimum residual and calculate the reduced χ^2_{red}), we can find the most conservative estimates of the external parameter uncertainties for χ^2_M statistics by multiplying the internal uncertainties by the coefficient $k_p t_{\max}$ [12].

Table 14 presents values of $\dfrac{\Delta_M(\gamma,\xi)}{\delta_1(\gamma)}$ calculated from our uncertainty intervals (and collected in Tables 2 and 4). $\delta_1 = 2\sigma_{est}$ is the uncertainty found using the differential-correction method. Note that the actual $\dfrac{\Delta_M(\gamma,\xi)}{2\sigma_{est}}$ ratio can change considerably for different realizations of the light curve (see the distribution density function in [12]). However, this theoretical function possesses an extremum, and the method suggested in [12] deals with the most probable ratio $\dfrac{\Delta_M(\gamma,\xi)}{2\sigma_{est}}$. For the light-curve of [2], the observed ratio $\dfrac{\Delta_M(\gamma,\xi)}{2\sigma_{est}}$ should be ∼2.6. Based upon the suggested method of [12], we conclude that the most probable theoretical value of $\dfrac{\Delta_M(\gamma,\xi)}{2\sigma_{est}}$ is ∼4. This exceeds the difference (derived from observations) between the uncertainties estimated using the differential-correction method and confidence-region method (with χ^2_M statistics) by a factor of ∼1.5. Nevertheless, using the most probable theoretical ratio of the intervals, $t_{max1} = \dfrac{\delta_M(\gamma,\xi)}{\delta_1(\gamma)}$ [12], enables us to avoid inconsistencies between parameters derived from different observations, which often arise for the differential-correction method (or Monte Carlo method), specify confidence intervals for the fitted parameters, and achieve a considerable reduction in the time required to calculate the uncertainty intervals.

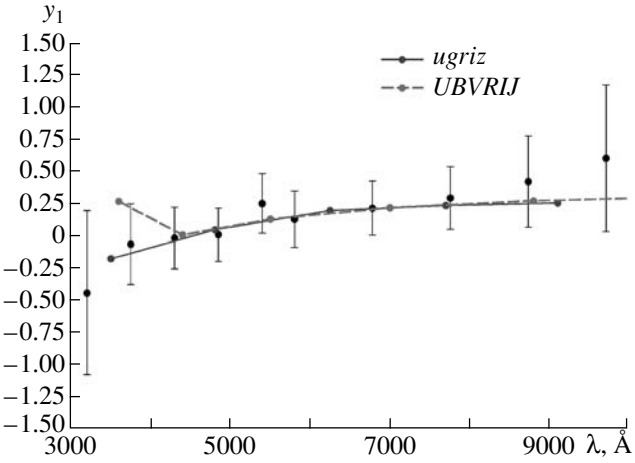

Fig. 10. Same as Fig. 9 for the limb-darkening coefficient y_1.

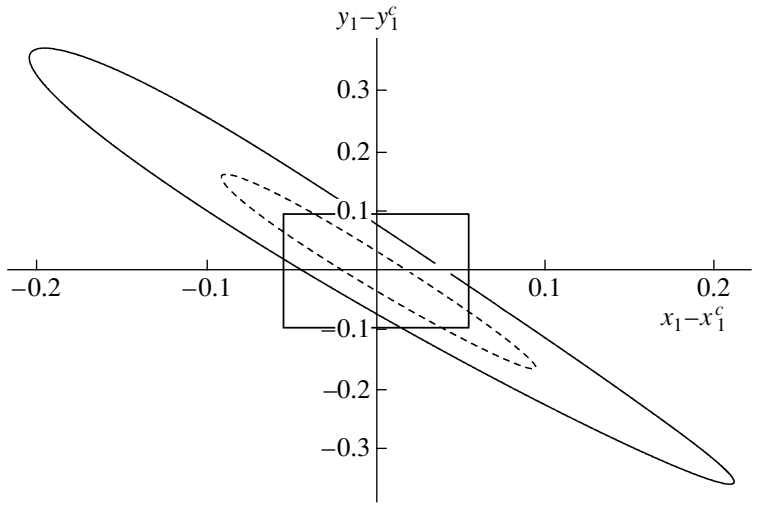

Fig. 11. Projection of the confidence region D (at the 95% confidence level) onto the (x_1, y_1) plane for the model with the quadratic limb-darkening law. The smaller ellipse (dashed curve) corresponds to the region found using χ^2_P statistics and the larger ellipse to the region found using χ^2_M statistics. The rectangle corresponds to the projection of the confidence region at the $2\sigma_{est}$ level found using the differential-correction method. The projection of the confidence region D is based on the observed light curve from [1].

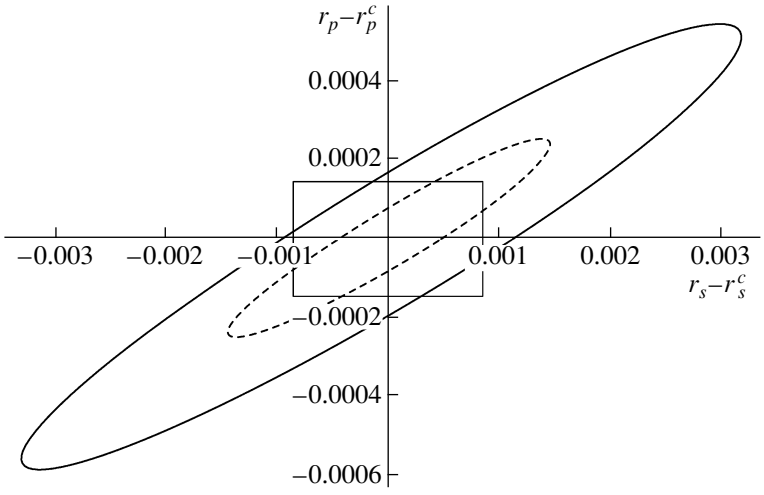

Fig. 12. Same as Fig. 11 for the projection of the confidence region D (at the 95% confidence level) onto the (r_p, r_s) plane.

8. CONCLUSIONS

We have determined the parameters of the system HD 209458 based on an analysis of high-precision satellite light curves of the eclipse of the star by the exoplanet. We have found the radii of the star and the exoplanet, the orbital inclination, and the linear and non-linear limb-darkening coefficients for the star. The derived parameters were analyzed in detail taking into account both internal and external parameter uncertainties, the latter being larger than the former by factors of two to four. Allowing for the external uncertainties makes it possible to reconcile the geometrical parameters derived from observations obtained at different wavelengths.

The relative radius of the exoplanet in the HD 209458 system (in units of the radius of the binary orbit) is $r_p = 0.01386$ (the mean value from Table 12). The optical star in HD 209458 is a G0V dwarf. This star's radius is $R_s = 7.98 \times 10^{10}$ cm (according to [2], assuming the star and planet masses are $M_s = 1.101 M_\odot$ and $M_p = 0.64 M_{Jup}$). Thus, the radius of the planet is $R_p = 9.70 \times 10^9$ cm. The planet's mass is [17] $M_p = 1.215 \times 10^{30}$ g, and its mean density is $\bar{\rho_p} = 0.318$ g cm^{-3}. Using the formula relating the surface gravity of the planet, g_p, and the radial-

velocity semi-amplitude of the star, K_s [5]:

$$g_p = \frac{2\pi}{P_{orb}} \frac{\left(1-e^2\right)^{1/2}\ K_s}{r_p^2 \sin i},$$

and substituting $e = 0$, $K_s = 85.1 \pm 1.0$ m/s [18], $P_{orb} = 3.52474859^{\rm d}$, and $i = 86.65°$ (Table 12), we find $g_p = 8.61$ m/s^2, close to that at the Earth's surface.

The ratio of the planet and star masses is $q = m_p/m_s = 0.00055$, and the planet's relative radius is $r_p = \dfrac{R_p}{a} = 0.01386$. To test our assumption that the planet is spherical, let us calculate the mean relative radius of the Roche lobe for the planet using the approximate formulas [19]

$$R_R = 0.49a \frac{q^{2/3}}{0.62q^{2/3} + \ln(1+q^{1/3})}, \qquad (27)$$

$$R_R = 0.46a \left(\frac{M_2}{M_1+M_2}\right)^{1/3}. \qquad (28)$$

Table 15 presents the mean relative radii of the Roche lobe, R_R/a (where a is the radius of the binary orbit) for various ratios of the planet and star masses, $q = m_p/m_s$, in the range $q = 0.00055-2$. The R_R/a values calculated from (27) and (28) are in good agreement, indicating that the estimate of the relative Roche-lobe radius for the planet is reliable. The radius of the planet is $r_p = 0.01386$ and that of its Roche lobe is $R_R/a = 0.039785$, so that the degree of filling of the planet's Roche lobe is $\mu = 0.35$, much less than 0.5. Thus, our assumption that the planet is spherical is quite justified (if we neglect a small amount of oblateness due to its axial rotation). The same is true for the optical star.

Information on the star's limb darkening is very valuable. Our analysis of the precise multi-color satellite light curves of Knutson et al. [2] has yielded wavelength dependences for the linear limb-darkening coefficient, $x(\lambda)$, as well as the non-linear limb-darkening coefficients in the quadratic law, $x_1(\lambda)$ and $y_1(\lambda)$. We confirm the difference between the observed and theoretical wavelength dependences for the linear limb-darkening coefficient x found by Southworth [5]. Our new result is that, even when the most conservative estimates of the external uncertainties in the limb-darkening coefficient x (with χ^2_M statistics) are used, there remains a significant discrepancy between the observed and theoretical $x(\lambda)$ relations. The observed $x(\lambda)$ are systematically below the theoretical values, with the difference increasing with wavelength, so that the observed linear limb-darkening coefficient is smaller than the theoretical one by a factor of about 1.5 at $\lambda \approx 9000$ Å. Thus, the stellar disk appears much more uniform in the red than is predicted by the theory of thin stellar atmospheres. The λ dependence for the limb-darkening coefficient x_1 in the quadratic law also differs significantly from the corresponding theoretical relation: the observed x_1 values are systematically below the theoretical ones, with difference increasing with wavelength λ. Note that this difference persists even when using the conservative external uncertainties of x_1 derived for χ^2_P statistics. The λ dependence of the limb-darkening coefficient y_1 in the quadratic law agrees with the corresponding theoretical relation within the errors.

Until recently, model stellar atmospheres were tested predominantly by comparing observed and theoretical spectra for the entire stellar disk. Precise satellite multi-color observations of exoplanet transits across stars provide a new unique possibility for independently checking model stellar atmospheres based on the angular distribution of the radiation exiting the star's atmosphere at different λ. An important advantage of eclipses of stars by exoplanets for determining stellar limb-darkening coefficients is that reflection and ellipsoidal effects are negligible and the eclipse is annular, with a relatively small radius for the eclipsing planet. Thus, despite the fact that the relative accuracy of the eclipse light curves is not extremely high ($\sim$1%–2% of the eclipse depth in the case of satellite observations), the above

Table 14. Observed ratios of the uncertainty interval Δ_M found in the confidence-region method with χ^2_M statistics ($\gamma = 0.95$) and the uncertainty $2\sigma_{est}$ estimated using the differential-correction method: the observed ratio $\dfrac{\Delta_M(\gamma,\xi)}{2\sigma_{est}}$ is presented for $k = r_s/r_p$, i, r_p, and r_s

λ, Å	k	r_s	r_p	i
3201	2.13	2.14	2.12	2.13
3750	2.30	2.31	2.29	2.30
4300	–	–	–	–
4849	2.00	2.00	2.00	2.00
5398	3.10	3.09	3.10	3.10
5802	–	–	–	–
6779	2.75	2.74	2.75	2.75
7755	2.36	2.35	2.37	2.36
8732	3.74	3.73	3.75	3.74
9708	–	–	–	–
Mean	2.63	2.62	2.63	2.63

Table 15. Dependence of the mean relative radius of the Roche lobe on the component-mass ratio calculated using (27) and (28)

Equation	q								
	0.00055	0.001	0.01	0.05	0.1	0.3	0.5	1	2
	R_R/a								
(27)	0.039785	0.048366	0.10201	0.16833	0.20677	0.28103	0.32079	0.37892	0.44000
(28)	0.037727	0.045985	0.098776	0.16673	0.20684	0.28215	0.31895	0.36510	0.40185

advantages make it possible to reliably determine the limb-darkening coefficients for both linear and nonlinear limb-darkening laws. Thus, such studies are important not only for determining the fundamental characteristics of exoplanets, but also for the further development of the theory of stellar atmospheres.

We note that Tutukov [20, 21] was the first to suggest the possibility of detecting eclipses of stars by exoplanets.

ACKNOWLEDGMENTS

The authors express special thanks to H.A. Knutson for providing his observations of HD 209458. This work was supported by the Russian Foundation for Basic Research (project 08-02-01220), the Program of State Support of Leading Scientific Schools of the Russian Federation (grant NSh-7179.2010.2), a grant from the President of Russia for the Support of Young Russian PhDs (grant MK-206.2009.2), and the analytic departmental program "Development of the Scientific Potential of Higher Education" (grant RNP-2.1.1.2906).

After our article was put to bed, we got acquainted with the article by A. Claret (Astron. Astrophys. **506**, 1335 (2009)) where the limb-darkening coefficients of the stellar disks were recalculated on the basis of Kurucz models. The new theoretical values of coefficients in the linear and nonlinear darkening law are close to previous ones (A. Claret, Astron. Astrophys. **428**, 1001 (2004)). Thereby, discrepancy between the observation of HD209458 and the theory is confirmed. Our work further shows that even using the most conservative estimates of the "external" parameters uncertainties, discrepancy between the observed and theoretical limb-darkening coefficients of star HD209458 is still significant.

REFERENCES

1. T. M. Brown, D. Charbonneau, R. L. Gilliland, et al., Astrophys. J. **552**, 699 (2001).
2. H. A. Knutson, D. Charbonneau, R. W. Noyes, et al., Astrophys. J. **655**, 564 (2007).
3. I. A. G. Shellen, E. J. W. de Mooij, and S. Albrecht, Nature **459**, 543 (2009).
4. *The CoRoT Space Mission: Early Results*, Ed. by C. Bertout, T. Forveille, N. Langer, and S. Shore, Astron. Astrophys. **506**, 1 (2009).
5. J. Southworth, Mon. Not. R. Astron. Soc. **386**, 1644 (2008).
6. A. Gimenez, Astron. Astrophys. **450**, 1231 (2006).
7. D. M. Popper and P. B. Etzel, Astron. J. **86**, 102 (1981).
8. J. Southworth, P. F. L. Maxted, and B. Smalley, Mon. Not. R. Astron. Soc. **351**, 1277 (2004).
9. D. M. Popper, Astron. J. **89**, 132 (1984).
10. A. M. Cherepashchuk, Astron. Zh. **70**, 1157 (1993) [Astron. Rep. **37**, 585 (1993)].
11. M. K. Abubekerov, N. Yu. Gostev, and A. M. Cherepashchuk, Astron. Zh. **85**, 121 (2008) [Astron. Rep. **52**, 99 (2008)].
12. M. K. Abubekerov, N. Yu. Gostev, and A. M. Cherepashchuk, Astron. Zh. **86**, 778 (2009) [Astron. Rep. **53**, 722 (2009)].
13. S. Wilks, *Mathematical Statistics* (Wiley, New York, 1967; Nauka, Moscow, 1967).
14. A. Burrows, I. Hubeny, J. Budai, and W. B. Hubbard, Astrophys. J. **661**, 502 (2007).
15. A. Claret, Astron. Astrophys. **428**, 1001 (2004).
16. F. Pont, H. Knutson, R. L. Gilliland, et al., Montly Notices of the Royal Astron. Soc. **385**, 109 (2008).
17. D. Charbonneau, T. M. Brown, D. W. Latham, and M. Mayor, Astrophys. J. **529**, L45 (2000).
18. D. Naef, M. Mayor, J. L. Beurit, et al., Astron. Astrophys. **414**, 351 (2004).
19. P. P. Eggleton, Astrophys. J. **268**, 368 (1983).
20. A. V. Tutukov, Astron. Zh. **69**, 1275 (1992) [Sov. Astron. **36**, 650 (1992)].
21. A. V. Tutukov, Astron. Zh. **72**, 400 (1995) [Astron. Rep. **39**, 354 (1995)].

Translated by N. Samus